Photoreforming of lignocellulose into H_2 using nano-engineered carbon nitride under benign conditions

Hatice Kasap‡, Demetra S. Achilleos‡, Ailun Huang, Erwin Reisner*

Christian Doppler Laboratory for Sustainable SynGas Chemistry, Department of Chemistry, University of Cambridge, Lensfield Road, Cambridge CB2 1EW, UK

Supporting Information Placeholder

ABSTRACT: Photoreforming of lignocellulose is a promising approach toward sustainable H_2 generation, but this kinetically challenging reaction currently requires UV-absorbing or toxic light absorbers under harsh conditions. Here, we report a cyanamide-functionalized carbon nitride, $^{NCN}CN_x$, which shows enhanced performance upon ultra-sonication. This activated $^{NCN}CN_x$ allows for the visible-light driven conversion of purified and raw lignocellulose samples into H_2 in the presence of various proton reduction co-catalysts. The reported room-temperature photoreforming process operates under benign aqueous conditions (pH ~2-15) without the need for toxic components.

Utilization of the most available form of biomass, lignocellulose, can provide sustainable and scalable H_2 fuel production, and its utilization does not impact on food production as it is an agricultural waste product.[1] the complex and energy-rich structure of lignocellulose is composed of cellulose, hemicellulose and lignin,[1,2] which have evolved to prevent degradation and are therefore kinetically challenging to utilize under ambient conditions.[3] Gasification at high-temperature (>750 °C) is a common method for H_2 production from lignocellulose, but energy-intensive and produces side products such as the fuel-cell inhibitor carbon monoxide.[4] Enzymatic hydrolysis is another process for biomass utilization, but this multistep conversion suffers from low overall yields.[3,5] Thus, there is substantial interest in developing novel approaches for the valorization of lignocellulose.[6–11]

Photoreforming of unprocessed biomass to H_2 has emerged as a clean alternative,[12,13] and it requires only a photocatalyst that generates holes to oxidize lignocellulose and electrons to drive proton reduction upon photoexcitation.[12] This process is traditionally carried out using UV-light harvesting TiO_2 modified with noble-metal catalysts such as RuO_2 and Pt.[14–16] Visible-light absorbing CdS quantum dots were recently reported for biomass photoreforming, but the system required toxic Cd and alkaline conditions (10 M KOH).[17] There is therefore a need to identify a photoreforming process that utilizes an inexpensive, non-toxic and visible-light absorbing photocatalyst, capable of operating under benign conditions.

Polymeric carbon nitride (CN_x) is a non-toxic and inexpensive carbonaceous photocatalyst.[18–20] The well-positioned band edges of CN_x give enough driving force for many photocatalytic reactions including proton reduction,[20–22] CO_2 reduction,[23,24] organic transformations (including alcohol oxidation),[25,26] redox catalysis[25,27] and water splitting.[28,29] Herein, we report a straightforward approach to enhance the photocatalytic performance of bulk cyanamide-functionalized carbon nitride ($^{NCN}CN_x$) by ultrasonication. The activated $^{NCN}CN_x$ is subsequently used to photoreform lignocellulosic biomass and generate H_2, in the presence of a molecular Ni bis(diphosphine) catalyst (**NiP**), heterogeneous Pt or MoS_2 in aqueous media over a range of pH values (Figures 1 and S1).

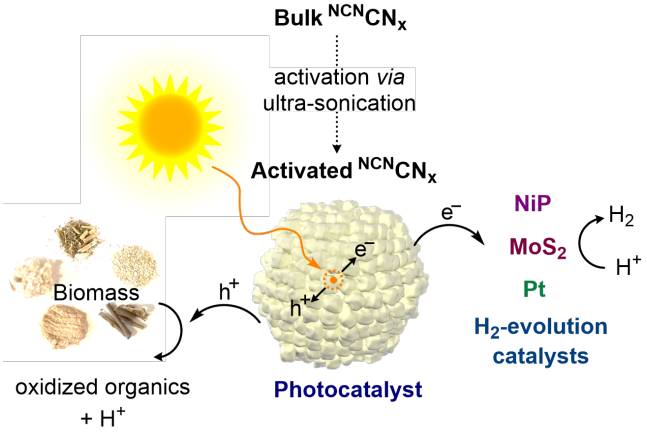

Figure 1. Schematic representation of H_2 generation through photoreforming of lignocellulose with $^{NCN}CN_x$ and H_2 production co-catalysts.

Bulk $^{NCN}CN_x$ was prepared and characterized as previously reported (see SI).[22,30] Activated $^{NCN}CN_x$ was obtained by ultra-sonicating an aqueous suspension of bulk $^{NCN}CN_x$ (5 mg mL^{-1}) in a potassium phosphate (KP_i) solution for 10 min at 40 ºC (Figure S2). UV-vis spectroscopy of the bulk and ultra-sonicated $^{NCN}CN_x$ reveals strong UV absorption, which tails into the visible region (λ_{abs} < 450 nm). A significant increase in absorbance is observed upon ultra-sonication of $^{NCN}CN_x$, which may be due to disruption of aggregated $^{NCN}CN_x$ and subsequently reduced light scattering and enhanced light absorption.[31] Photoluminescence studies (λ_{ex} = 360 nm) also reveal an increased emission intensity for the ultra-sonicated $^{NCN}CN_x$, possibly suggesting a higher density of photoexcited states. Brunauer–Emmett-Teller measurements show a 60% increase in the surface area after ultra-sonication (97.4±0.6 m^2 g^{-1}),[32]

and a smaller aggregate size following ultra-sonication is confirmed by Transmission Electron Microscopy (TEM) and Scanning Electron Microscopy (SEM). Nearly identical X-ray diffraction patterns and Fourier Transform Infrared spectra are observed, indicating that the characteristic functional group features of ^{NCN}**CN$_x$** are preserved after ultra-sonication (Figure S2).[22,33]

A photocatalytic screening assay was carried out by dispersing ^{NCN}**CN$_x$** in KP$_i$ (pH 4.5) solution containing a DuBois-type Ni proton reduction catalyst (**NiP**; Figure S1),[34] with 4-methyl benzyl alcohol (4-MBA, 30 µmol).[25] 4-MBA was selected as the electron donor as it is as an easily oxidized model cellulose substrate. The samples were irradiated under a N_2 atmosphere with simulated solar light (100 mW cm^{-2}, AM1.5G, 25 °C). The reaction conditions were optimized systematically with respect to ^{NCN}**CN$_x$**-based H_2 production activity (specific activity; µmol H_2 (g ^{NCN}**CN$_x$**)$^{-1}$ h^{-1}), **NiP**-based activity represented by Ni-based turnover frequency (TOF$_{NiP}$; mol H_2 (mol **NiP**)$^{-1}$ h^{-1}) and turnover number (TON$_{NiP}$; mol H_2 (mol **NiP**)$^{-1}$), and overall proton reduction and alcohol oxidation rates (Tables S1-S7).

The results of photoreforming 4-MBA using 0.5 mg bulk and activated ^{NCN}**CN$_x$** with 300 nmol of **NiP** are shown in Figure 2. After 1 h of irradiation, activated ^{NCN}**CN$_x$** shows more than three times the photocatalytic activity of bulk ^{NCN}**CN$_x$**, reaching 17.2±0.6 µmol H_2 h^{-1}, TOF$_{NiP}$ of 57.5±2.1 h^{-1} and 34480±1240 µmol H_2 (g ^{NCN}**CN$_x$**)$^{-1}$ h^{-1}. Quantitative and selective oxidation of 4-MBA into 4-methyl benzaldehyde (4-MBAd) is observed in less than 6 h irradiation. A specific activity of 39310±1970 µmol H_2 (g ^{NCN}CN$_x$)$^{-1}$ h^{-1} is reached with 0.5 mg activated ^{NCN}**CN$_x$** and 400 nmol of **NiP** (Figure S3 and S4), which represents a benchmark H_2 evolution rate for a CN$_x$ photocatalyst.[35,36] Control experiments in the absence of ^{NCN}**CN$_x$**, **NiP**, 4-MBA or light did not produce H_2 (Table S6). The external quantum efficiencies (EQE; λ = 360±10 nm) yielded (22±1)% and (13±1)% for the activated and bulk systems, respectively.

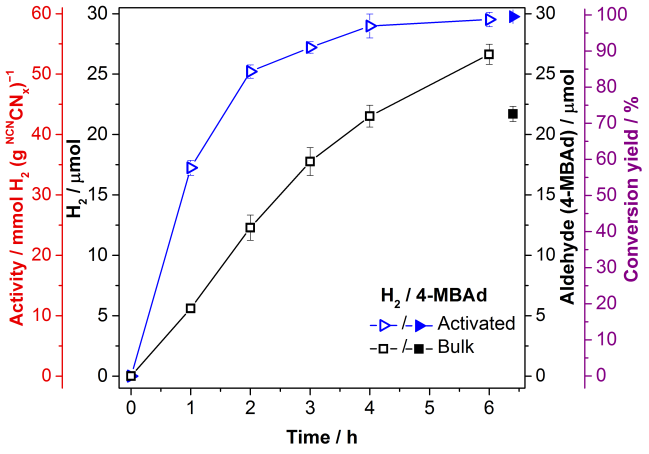

Figure 2. Photocatalytic H_2 and 4-MBAd formation using activated and bulk ^{NCN}**CN$_x$** (0.5 mg) with **NiP** (300 nmol) in KP$_i$ (0.1 M, pH 4.5, 3 mL) with 4-MBA (30 µmol) under AM1.5G irradiation at 25 °C (hollow symbols refer to H_2 generation; filled symbols to MBAd production).

We have previously shown that ^{NCN}**CN$_x$** can photo-charge and accumulate trapped electrons with a very long life-time in the presence of 4-MBA.[25,37] The density of accumulated charges remain approximately the same for bulk and activated ^{NCN}**CN$_x$**, but activated ^{NCN}**CN$_x$** shows a faster discharging behavior (Figure S5 and Table S7), indicating that the co-catalyst can more easily access electrons stored in CN$_x$.

4-MBA was subsequently replaced with purified lignocellulose components. α-cellulose was initially selected as the most abundant form of wood-derived biomass and the most unreactive form of cellulose.[38] The reaction conditions were optimized for the overall amount of H_2 being produced by varying the amount of α-cellulose, activated ^{NCN}**CN$_x$** and **NiP** loadings (Table S8, Figures S6-S7). The system containing 0.5 mg ^{NCN}**CN$_x$** and 50 nmol **NiP** photo-produced 1690±100 µmol H_2 (g ^{NCN}**CN$_x$**)$^{-1}$ h^{-1} and TOF$_{NiP}$ of 17.0±1.1 h^{-1}. The highest overall H_2 production yield of 2.62±0.09 µmol H_2 was observed with 5 mg activated ^{NCN}**CN$_x$** and 50 nmol **NiP** in KP$_i$ (pH 4.5) after 4 h of AM 1.5G irradiation. UV-filtered simulated solar light (λ > 400 nm) produced 1.10±0.03 µmol of H_2, indicating efficient utilization of visible light. The importance of surface-functionalization for cellulose photoreforming is highlighted by the negligible activity of unfunctionalized bulk ^{H_2N}**CN$_x$** (only 0.13±0.04 µmol H_2) and reduced performance of bulk ^{NCN}**CN$_x$** (1.91±0.07 µmol H_2) after 4 h of UV-vis irradiation (Figure S8).[25] This significant difference in activity has been previously attributed to the superior oxidizing ability of ^{NCN}**CN$_x$** due to more positively positioned valence band (+2.2 V *vs.* NHE at pH 6; band gap of 2.7 eV),[39] as well as improved hole transfer to the electron donor via the cyanamide moieties.[25,30,40]

Photocatalytic biomass reformation into H_2 was then expanded to xylan and lignin as well as the most common units found in their structures (Figure 3, Table S9). As the substrate size is reduced, solubility improves in pH 4.5 KP$_i$, resulting in significantly enhanced photoactivity. After 24 h of irradiation, up to 32.1±4.8 µmol of H_2 was produced from glucose at 1120±80 µmol H_2 (g ^{NCN}**CN$_x$**)$^{-1}$ h^{-1} and TOF$_{NiP}$ of 112±8 h^{-1}. In the presence of xylose and galactose monosaccharides, 19.9±2.3 and 28.0±2.5 µmol of H_2 were produced respectively after 24 h of irradiation. Photoreforming of polymeric xylan generated 4.92±0.17 µmol of H_2. Despite the strong light absorbing nature and robustness of lignin, 0.20±0.03 µmol H_2 production was achieved, with TOF$_{NiP}$ of 4.0±0.7 h^{-1} and 40.8±6.8 µmol H_2 (g ^{NCN}**CN$_x$**)$^{-1}$ h^{-1}. The results demonstrate that the system photoreforms biomass under mildly acidic aqueous conditions, but is still limited by substrate availability to quench photogenerated holes in ^{NCN}**CN$_x$**.

Replacement of purified lignocellulosic components with raw and unprocessed 'real-world' biomass samples (Figure S9, Table S10) resulted in H_2 formation with a range of samples (including paper and cardboard). Sawdust produced 3.89±0.34 µmol of H_2 with TOF$_{NiP}$ of 20.2±0.4 h^{-1} and 202±4 µmol H_2 (g ^{NCN}**CN$_x$**)$^{-1}$ h^{-1} upon irradiation using ^{NCN}**CN$_x$** in KP$_i$ solution.

The long-term performance of the system was investigated by comparing the activity of **NiP** with benchmark proton reduction co-catalysts, Pt and MoS_2 (Figure 4a, Table S11) in the presence of α-cellulose.[22,41] **NiP** shows a superior initial rate, but the fragile molecular framework degrades after 24 h,[42] producing 3.7±0.1 µmol of H_2 with ^{NCN}**CN$_x$-NiP**. Instead, Pt and MoS_2 display slower kinetics, but a much-enhanced stability while photocatalytic systems with Pt are still active after twelve days.

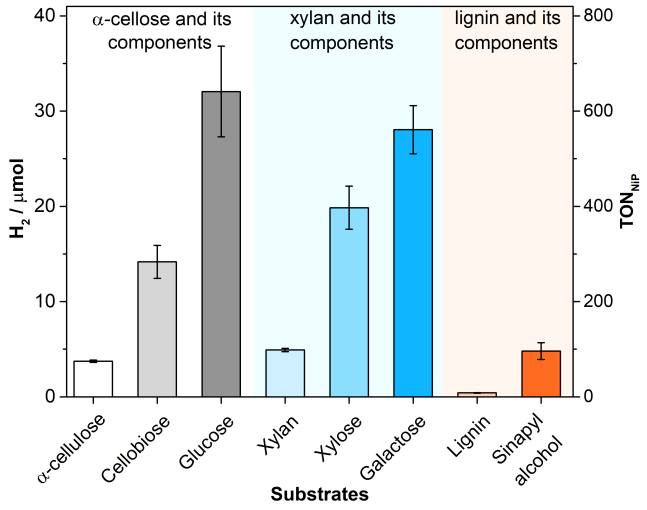

Figure 3. Photocatalytic H_2 production using activated $^{NCN}\mathbf{CN_x}$ (5 mg) and **NiP** (50 nmol) with purified lignocellulose components (100 mg) in KP_i solution (0.1 M, pH 4.5, 3 mL) under AM1.5G irradiation for 24 h at 25 °C.

Mass spectrometry of the photocatalytic samples prepared in H_2O and D_2O confirms that H_2 production originates from the aqueous protons (Figure S10, Table S12). The oxidation products were characterized after photoreformation of uniformly ^{13}C-labelled cellulose over activated $^{NCN}\mathbf{CN_x}$ (5 mg) and Pt (4 wt.%) in pH 4.5 KP_i solution prepared in D_2O using ^{13}C-NMR spectroscopy. ^{13}C-NMR spectroscopy of the filtered solution shows the formation of formate (δ = 171 ppm) and carboxylate groups (δ = 183 ppm) of presumably lower molecular weight polysaccharides (δ = 50-110 ppm; Figure S11).[17,43] Other gaseous oxidation products in the headspace were monitored by gas chromatography and mass spectrometry after 6 days of irradiation (Figure S12, Table S13). Negligible amounts of CO and CO_2 were measured, which is in agreement with the insignificant quantities of carbonate detected by ^{13}C-NMR spectroscopy. The oxidation is likely to occur directly *via* hole transfer due to strong binding between the lignocellulosic substrates and $^{NCN}\mathbf{CN_x}$ as photogenerated holes in $^{NCN}\mathbf{CN_x}$ are not oxidizing enough to produce $HO^{\bullet}$.[17,25,30]

The versatility of the system was investigated by suspending α-cellulose in 1, 5, 10 M KOH (~pH 14-15), KP_i solution (pH 4.5, pH 7) and H_2SO_4 (pH 2) during stirring for 24 h at 25 °C prior to addition of H_2PtCl_6 (4 wt.%) and activated $^{NCN}\mathbf{CN_x}$ (Figure 4b, Table S14). After six days of irradiation under 10 M KOH conditions, 39.5±1.1 µmol of H_2 was produced, which is twice the H_2 production yield observed in 5 M KOH. 1 M KOH, H_2SO_4 and pH 7 KP_i solution all resulted in H_2 production yields comparable to that of a pH 4.5 KP_i solution. These activities are consistent with the higher solubility of cellulose under alkaline conditions (Figure S13, Table S15).[44,45] The conversion yield determined with different α-cellulose loadings indicates that 22% conversion is reached after six days of irradiation in 10 M KOH solution (Table S16),[46] more than twice the yield reported for CdS/CdO_x quantum dots under similar conditions (9.7%).[17]

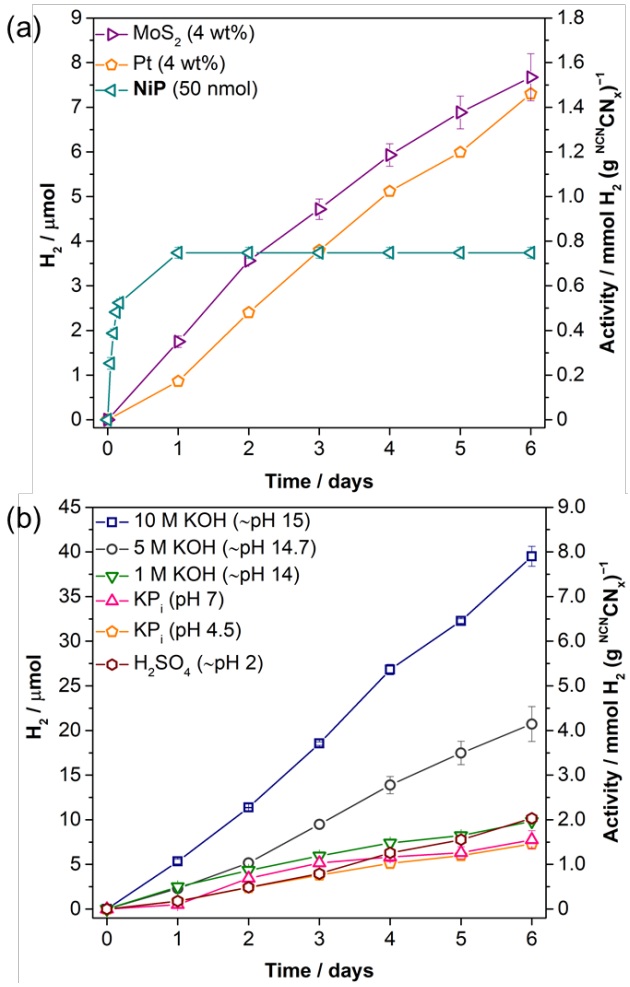

Figure 4. (a) H_2 production using activated $^{NCN}\mathbf{CN_x}$ (5 mg), α-cellulose (100 mg) in KP_i (0.1 M, pH 4.5, 3 mL) under AM1.5G irradiation with different co-catalysts; **NiP** (50 nmol), H_2PtCl_6 (4 wt.%) or $H_8N_2MoS_4$ (4 wt.%). (b) Photocatalytic H_2 production using activated $^{NCN}\mathbf{CN_x}$ (5 mg) with H_2PtCl_6 (4 wt.%) and α-cellulose (100 mg) in different media; 1, 5, 10 M KOH (pH 14-15), H_2SO_4 (pH 2) or KP_i (pH 4.5 and pH 7).

In summary, we report a straightforward ultra-sonication approach to breakdown aggregates of $^{NCN}\mathbf{CN_x}$, which results in enhanced photoactivity. The activated $^{NCN}\mathbf{CN_x}$ reaches 39310±1970 µmol H_2 (g $^{NCN}CN_x)^{-1}$ h^{-1} for the photoreforming of 4-MBA. Both purified lignocellulosic components and raw biomass substrates are photoreformed to H_2 with activated $^{NCN}\mathbf{CN_x}$ and **NiP** in KP_i (pH 4.5) at 25 °C, demonstrating precious metal-free, non-toxic and visible light-promoted photoreforming of biomass under benign conditions. Activated $^{NCN}\mathbf{CN_x}$ functions with molecular and heterogeneous co-catalysts, with high stability and a range of pH values, although alkaline conditions still exhibit the best performance and highest conversion yield. The utilization of a carbon-based photocatalyst for photoreforming of biomass offers new perspectives for clean H_2 fuel production from waste sources, with prospects to extract valuable chemicals from the oxidation process in future development.

ASSOCIATED CONTENT

Supporting Information

The Supporting Information is available free of charge on the ACS Publications website.

Experimental Section, Supporting Tables S1 to S16 and Supporting Figures S1 to S13 (PDF).

AUTHOR INFORMATION

Corresponding Author

*reisner@ch.cam.ac.uk

Author Contributions

‡These authors contributed equally.

Competing interest

A patent application on the reported work has been filed (UK patent application number GB1808905.2), which lists HK, DSA and ER as inventors.

ACKNOWLEDGMENT

This work was financially supported by the Austrian Federal Ministry for Digital and Economic Affairs, the National Foundation for Research, Technology and Development and OMV. We acknowledge help from Dr. Heather F. Greer for recording the SEM and TEM images and thank Mr. Xin Fang for his help in preparing artwork.

REFERENCES

(1) Isikgor, F. H.; Becer, C. R. *Polym. Chem.* **2015**, *6*, 4497–4559.
(2) Hendriks, A. T. W. M.; Zeeman, G. *Bioresour. Technol.* **2009**, *100*, 10–18.
(3) Himmel, M. E.; Ding, S.-Y.; Johnson, D. K.; Adney, W. S.; Nimlos, M. R.; Brady, J. W.; Foust, T. D. *Science* **2007**, *315*, 804–807.
(4) Sikarwar, V. S.; Zhao, M.; Clough, P.; Yao, J.; Zhong, X.; Memon, M. Z.; Shah, N.; Anthony, E. J.; Fennell, P. S. *Energy Environ. Sci.* **2016**, *9*, 2939–2977.
(5) Himeshima, N.; Amao, Y. *Green Chem.* **2005**, *7*, 742–746.
(6) Reichert, J.; Brunner, B.; Jess, A.; Wasserscheid, P.; Albert, J. *Energy Environ. Sci.* **2015**, *8*, 2985–2990.
(7) Albert, J.; Jess, A.; Kern, C.; Pöhlmann, F.; Glowienka, K.; Wasserscheid, P. *ACS Sustain. Chem. Eng.* **2016**, *4*, 5078–5086.
(8) Zhang, P.; Guo, Y.-J.; Chen, J.; Zhao, Y.-R.; Chang, J.; Junge, H.; Beller, M.; Li, Y. *Nat. Catal.* **2018**, *1*, 332–338.
(9) Grande, P. M.; Viell, J.; Theyssen, N.; Marquardt, W.; Domínguez de María, P.; Leitner, W. *Green Chem.* **2015**, *17*, 3533–3539.
(10) Zinoviev, S.; Müller-Langer, F.; Das, P.; Bertero, N.; Fornasiero, P.; Kaltschmitt, M.; Centi, G.; Miertus, S. *ChemSusChem* **2010**, *3*, 1106–1133.
(11) Albert, J.; Wölfel, R.; Bösmann, A.; Wasserscheid, P. *Energy Environ. Sci.* **2012**, *5*, 7956–7962.
(12) Puga, A. V. *Coord. Chem. Rev.* **2016**, *315*, 1–66.
(13) Kuehnel, M. F.; Reisner, E. *Angew. Chem. Int. Ed.* **2018**, *57*, 3290–3296.
(14) Kawai, T.; Sakata, T. *Nature* **1980**, *286*, 474–476.
(15) Speltini, A.; Sturini, M.; Dondi, D.; Annovazzi, E.; Maraschi, F.; Caratto, V.; Profumo, A.; Buttafava, A. *Photochem. Photobiol. Sci.* **2014**, *13*, 1410–1419.
(16) Caravaca, A.; Jones, W.; Hardacre, C.; Bowker, M. *Proc. R. Soc. A* **2016**, *472*, 20160054.
(17) Wakerley, D. W.; Kuehnel, M. F.; Orchard, K. L.; Ly, K. H.; Rosser, T. E.; Reisner, E. *Nat. Energy* **2017**, *2*, 17021.
(18) Cao, S.; Low, J.; Yu, J.; Jaroniec, M. *Adv. Mater.* **2015**, *27*, 2150–2176.
(19) Antonietti, M.; Oschatz, M. *Adv. Mater.* **2018**, *30*, 1706836.
(20) Wang, X.; Maeda, K.; Thomas, A.; Takanabe, K.; Xin, G.; Carlsson, J. M.; Domen, K.; Antonietti, M. *Nat. Mater.* **2009**, *8*, 76–80.
(21) Caputo, C. A.; Gross, M. A.; Lau, V. W-h.; Cavazza, C.; Lotsch, B. V.; Reisner, E. *Angew. Chem. Int. Ed.* **2014**, *53*, 11538–11542.
(22) Lau, V. W.-h; Moudrakovski, I.; Botari, T.; Weinberger, S.; Mesch, M. B.; Duppel, V.; Senker, J.; Blum, V.; Lotsch, B. V. *Nat. Commun.* **2016**, *7*, 12165.
(23) Kuriki, R.; Yamamoto, M.; Higuchi, K.; Yamamoto, Y.; Akatsuka, M.; Lu, D.; Yagi, S.; Yoshida, T.; Ishitani, O.; Maeda, K. *Angew. Chem. Int. Ed.* **2017**, *56*, 4867–4871.
(24) Cometto, C.; Kuriki, R.; Chen, L.; Maeda, K.; Lau, T.-C.; Ishitani, O.; Robert, M. *J. Am. Chem. Soc.* **2018**, *140*, 7437–7440.
(25) Kasap, H.; Caputo, C. A.; Martindale, B. C. M.; Godin, R.; Lau, V. W.-h; Lotsch, B. V.; Durrant, J. R.; Reisner, E. *J. Am. Chem. Soc.* **2016**, *138*, 9183–9192.
(26) Zhao, Y.; Shalom, M.; Antonietti, M. *Appl. Catal. B Environ.* **2017**, *207*, 311–315.
(27) Yang, P.; Wang, R.; Zhou, M.; Wang, X. *Angew. Chem. Int. Ed.* **2018**, *57*, 8674–8677.
(28) Liu, J.; Liu, Y.; Liu, N.; Han, Y.; Zhang, X.; Huang, H.; Lifshitz, Y.; Lee, S.-T.; Zhong, J.; Kang, Z. *Science* **2015**, *347*, 970–974.
(29) Zhang, G.; Lan, Z.-A.; Lin, L.; Lin, S.; Wang, X. *Chem. Sci.* **2016**, *7*, 3062–3066.
(30) Kasap, H.; Godin, R.; Jeay-Bizot, C.; Achilleos, D. S.; Fang, X.; Durrant, J. R.; Reisner, E. *ACS Catal.* **2018**, *8*, 6914–6926.
(31) Wu, M.; Yan, J.-M.; Zhang, X.-W.; Zhao, M.; Jiang, Q. *J. Mater. Chem. A* **2015**, *3*, 15710–15714.
(32) Lau, V. W.-h; Yu, V. W.; Ehrat, F.; Botari, T.; Moudrakovski, I.; Simon, T.; Duppel, V.; Medina, E.; Stolarczyk, J. K.; Feldmann, J.; Blum, V.; Lotsch, B. V. *Adv. Energy Mater.* **2017**, *7*, 1602251.
(33) Horvath-Bordon, E.; Kroke, E.; Svoboda, I.; Fuess, H.; Riedel, R. *New J. Chem.* **2005**, *29*, 693–699.
(34) Gross, M. A.; Reynal, A.; Durrant, J. R.; Reisner, E. *J. Am. Chem. Soc.* **2014**, *136*, 356–366.
(35) Martin, D. J.; Qiu, K.; Shevlin, S. A.; Handoko, A. D.; Chen, X.; Guo, Z.; Tang, J. *Angew. Chem. Int. Ed.* **2014**, *53*, 9240–9245.
(36) Han, Q.; Cheng, Z.; Wang, B.; Zhang, H.; Qu, L. *ACS Nano* **2018**, *12*, 5221–5227.
(37) Lau, V. W.-h; Klose, D.; Kasap, H.; Podjaski, F.; Pignié, M.-C.; Reisner, E.; Jeschke, G.; Lotsch, B. V. *Angew. Chem. Int. Ed.* **2017**, *56*, 510–514.
(38) Sun, Y.; Cheng, J. *Bioresour. Technol.* **2002**, *83*, 1–11.
(39) Meyer, A. U.; Lau, V. W.-h; König, B.; Lotsch, B. V. *European J. Org. Chem.* **2017**, *2017*, 2179–2185.
(40) Ou, H.; Chen, X.; Lin, L.; Fang, Y.; Wang, X. *Angew. Chem. Int. Ed.* **2018**, *57*, 8729–8733.
(41) Gu, Q.; Sun, H.; Xie, Z.; Gao, Z.; Xue, C. *Appl. Surf. Sci.* **2017**, *396*, 1808–1815.
(42) Martindale, B. C. M.; Joliat, E.; Bachmann, C.; Alberto, R.; Reisner, E. *Angew. Chem. Int. Ed.* **2016**, *55*, 9402–9406.
(43) Ramos, M. L.; Caldeira, M. M.; Gil, V. M. S. *Carbohydr. Res.* **1997**, *304*, 97–109.
(44) Budtova, T.; Navard, P. *Cellulose* **2016**, *23*, 5–55.
(45) Medronho, B.; Romano, A.; Miguel, M. G.; Stigsson, L.; Lindman, B. *Cellulose* **2012**, *19*, 581–587.
(46) Zhang, G.; Ni, C.; Huang, X.; Welgamage, A.; Lawton, L. A.; Robertson, P. K. J.; Irvine, J. T. S. *Chem. Commun.* **2016**, *52*, 1673–1676.

Table of Contents